

Electron-nuclear double resonance of $^{57}\text{Fe}^{3+}$ in RbAl and RbGa sulfate alums

J. R. Brisson and A. Manoogian

Department of Physics, University of Ottawa, Ottawa K1N 9B4, Canada

(Received 28 March 1978)

The electron-nuclear double resonance (ENDOR) of the S -state ion $^{57}\text{Fe}^{3+}$ is studied in the trigonally distorted octahedral sites of the hydrated crystals $\text{RbAl}(\text{SO}_4)_2 \cdot 12\text{H}_2\text{O}$ and $\text{RbGa}(\text{SO}_4)_2 \cdot 12\text{H}_2\text{O}$. ENDOR frequencies from all four inequivalent sites in the unit cell of the crystals were measured and fitted to an appropriate spin Hamiltonian, which included higher-order trigonal terms of the type S^3I . Exact diagonalization of the spin Hamiltonian expressed in trigonal symmetry adequately described the observed frequencies for measurements with the magnetic field along two directions in the crystals.

I. INTRODUCTION

The electron-nuclear double resonance (ENDOR) of $^{57}\text{Fe}^{3+}$ dopant S -state ions is studied in single crystals of $\text{RbAl}(\text{SO}_4)_2 \cdot 12\text{H}_2\text{O}$ and $\text{RbGa}(\text{SO}_4)_2 \cdot 12\text{H}_2\text{O}$ alums. In the Rb sulfate alums the octahedral-crystal-field splitting of the $\text{Fe}^{3+} \cdot 6\text{H}_2\text{O}$ magnetic complexes is of the same order of magnitude as the trigonal-field splitting. The purpose of this study is to obtain accurate values of the Fe hyperfine parameters in hydrated crystals, since they should be of importance in classifying the physical behavior of such systems. The normal abundance of ^{57}Fe ($I = \frac{1}{2}$) is $\sim 2\%$, but in this work the isotope enriched to $\sim 96\%$ was used to obtain large-intensity hyperfine lines on which to perform the ENDOR measurements. All the measurements were done at X -band microwave frequency (~ 9.4 GHz) and at a temperature of 4.2 K using a spectrometer described previously.¹

The ENDOR of $^{57}\text{Fe}^{3+}$ has been previously reported in the crystals MgO ,² CaO ,³ and SnO .⁴ The crystalline electric field at the Fe site in MgO and CaO is of octahedral symmetry, while in SnO it is strongly rhombic. Culvahouse and Olsen⁵ grew hydrated double nitrate crystals doped with the enriched isotope $^{57}\text{Fe}^{3+}$, and the ESR spectra showed resolved hyperfine structure. The crystalline electric field at the Fe site in the double nitrate crystal is of trigonal symmetry, and a value of $|A| = (10.9 \pm 0.3) \times 10^{-4} \text{ cm}^{-1}$ was reported for the hyperfine parameter. The values of the hyperfine parameters measured in this work using the ENDOR technique are improved by two significant figures over the ordinary ESR method, and the asymmetry of the parameters is also determined. Moreover, additional trigonal terms of the type S^3I are also required in the spin Hamiltonian to adequately describe the observed ENDOR frequencies. The ESR spectrum of Fe^{3+} in $\text{RbAl}(\text{SO}_4)_2 \cdot 12\text{H}_2\text{O}$ alum was studied by

Bleaney and Trenam,⁶ but $\text{RbGa}(\text{SO}_4)_2 \cdot 12\text{H}_2\text{O}$ was not studied. The sign of the cubic field splitting parameter a was reported to be negative in the Rb alum, but Geschwind⁷ later showed that it was positive. Watanabe⁸ showed from theoretical considerations that the sign of a is probably always positive in any cubic environment.

In the families of hydrated crystals which possess a trigonal distortion at the trivalent ion site, namely the sulfate alums, guanidinium aluminum sulfate hexahydrate (GASH) and its isomorphs, and $\text{AlCl}_3 \cdot 6\text{H}_2\text{O}$, the trigonal distortion of the $\text{Fe}^{3+} \cdot 6\text{H}_2\text{O}$ magnetic complexes is usually very large, and the trigonal term in the spin Hamiltonian gives the dominant contribution to the crystal-field splitting. The Rb sulfate alums are an exception in that they possess a small trigonal distortion that produces a crystal-field splitting of the same order of magnitude as the cubic crystal field. From the previous ESR studies of Fe^{3+} in RbAl and KAl(Se) alums,⁶ it is noted that the (corrected) sign of the trigonal-crystal-field splitting parameter D is negative for RbAl alum and positive for KAl(Se) alum. Also, the magnitude of D increases with decreasing temperature in both cases. Hence in a plot of D versus temperature for the Fe-doped alums the curves are bent toward the temperature axis.

In the classification of the chromium-doped alums,⁹ it was found that the chromium D parameter was positive for the Rb sulfate alums and negative for the Cs sulfate alums. The positive sign was related to a trigonal extension of the octahedron of water molecules coordinated to the Cr ion, and the negative sign was related to compression. The magnitude of D was found to decrease with decreasing temperature in both cases. Hence in a plot of D versus temperature for the Cr-doped alums the curves are bent away from the temperature axis. The magnitude of the chromium D parameter was found to be greater in RbGa than in RbAl alum, but it was smaller in

CsGa than in CsAl alum. This effect is believed to be a consequence of the Cr ion being in a trigonally extended environment in the Rb alums, and in a compressed one in the Cs alums.

In the unit cell of the alums there are four identical trigonally distorted octahedral arrays of water molecules containing a trivalent ion. The trigonal axes of the octahedra coincide with the crystal $\langle 111 \rangle$ body diagonals, and so the four magnetic complexes are inequivalent. The positions of the water molecules forming the octahedra define the cubic field axes directions, and, in the Rb alums, these directions are displaced from the crystal $\langle 100 \rangle$ directions by a small rotation of the octahedra about the body diagonals. For small

rotations the positions of the cubic field axes will be close to the $\{100\}$ crystal planes. The Fe^{3+} dopant ion substitutes for Al^{3+} and Ga^{3+} ions in the respective alums.

II. EXPERIMENTAL

A. ESR results

Bleaney and Trenam⁶ analyzed the Fe^{3+} ESR fine-structure spectrum in RbAl alum in terms of a spin Hamiltonian relative to the cubic field axes. In this work the following spin Hamiltonian, reflecting the trigonal symmetry of the octahedral sites, is used¹⁰:

$$\mathcal{H} = g\mu_B H \cos\theta S_z + \frac{1}{2}g\mu_B H \sin\theta(S_+ + S_-) + D[S_z^2 - \frac{1}{3}S(S+1)] - \frac{1}{180}(a-F)[35S_z^4 - 30S(S+1)S_z^2 + 25S_z^2 - 6S(S+1) + 3S^2(S+1)^2] + \frac{1}{36}(a\sqrt{2})[S_x(S_z^2 e^{i3(\phi-\alpha)} + S_z^2 e^{-i3(\phi-\alpha)}) + (S_x^3 e^{i3(\phi-\alpha)} + S_x^3 e^{-i3(\phi-\alpha)})S_z], \quad (1)$$

where $S_+ = S_x + iS_y$ and $S_- = S_x - iS_y$.

In Eq. (1) the z axis is along a $\langle 111 \rangle$ direction and the x axis is chosen to coincide with the projection of \vec{H} on a plane perpendicular to the z axis. The angles are defined as follows: θ is the angle between the \vec{H} and z directions; α is the angle of rotation of the octahedron about the z axis; and ϕ is the angle between the projection of \vec{H} in the trigonal plane and the projection of the $[001]$ axis in the same plane (a $\langle 112 \rangle$ axis).

The magnetic field positions H , for resonance at a fixed microwave frequency ν , are given to second order in perturbation theory by the expressions

$$\begin{aligned} \pm \frac{5}{2} \rightarrow \pm \frac{3}{2} : g\mu_B H &= h\nu \mp 2D[(3 \cos^2\theta - 1) + 2pa + \frac{1}{6}Fq] \\ &\quad - 32\delta_1 + 4\delta_2 + \epsilon_1, \\ \pm \frac{3}{2} \rightarrow \pm \frac{1}{2} : g\mu_B H &= h\nu \mp D[(3 \cos^2\theta - 1) - \frac{5}{2}pa - \frac{5}{24}Fq] \\ &\quad + 4\delta_1 - 5\delta_2 + \epsilon_2, \end{aligned} \quad (2)$$

$$\frac{1}{2} \rightarrow -\frac{1}{2} : g\mu_B H = h\nu + 16\delta_1 - 8\delta_2 + \epsilon_3,$$

where

$$\begin{aligned} p &= -\frac{1}{12}q + \frac{1}{3}5\sqrt{2}\sin^3\theta \cos\theta \cos(\phi - \alpha), \\ q &= 35\cos^4\theta - 30\cos^2\theta + 3, \\ \delta_1 &= (D^2/h\nu)\cos^2\theta \sin^2\theta, \quad \delta_2 = (D^2/h\nu)\sin^4\theta, \\ \epsilon_1 &= (a^2/h\nu)[\frac{5}{3}\sigma(1 - 7\sigma)], \\ \epsilon_2 &= -(a^2/h\nu)[\frac{5}{48}(3 + 178\sigma - 625\sigma^2)], \\ \epsilon_3 &= (a^2/h\nu)[\frac{10}{3}\sigma(7 - 25\sigma)], \end{aligned}$$

and

$$\sigma = \frac{1}{5}(1 - p).$$

Hence, with the magnetic field in a general direction, these expressions describe 20 ESR lines corresponding to the allowed transitions $\Delta M_s = \pm 1$, five lines for each inequivalent site.

The ESR spectra for Fe^{3+} in RbAl and RbGa sulfate alums are quite similar, the chief difference being the larger trigonal-field splitting in RbGa alum. To evaluate the fine-structure parameters in the spin Hamiltonian, measurements were taken along a trigonal axis, which is the $[111]$ axis, at a cubic field axis and in a $[1\bar{1}0]$ direction. To obtain measurements near a cubic field axis, the magnet was rotated a small angle from the $[100]$ direction in the (110) plane to the position where the magnetic field separation between the ESR lines was a maximum. For H on a given $[111]$ axis the trigonal axes of the remaining three sites all make angles of 70.5° with the applied field and their spectra coincide. For H along the $[1\bar{1}0]$ direction two trigonal axes make angles of 90° with the field, and two make angles of 36° . Hence the spectral lines in this direction are in pairs. For H near a cubic field axis 20 lines should be observed, but it was possible to measure only about nine of them because of incomplete resolution due to overlapping of lines. Typical ESR spectra obtained in RbGa alum are shown in Fig. 1. The hyperfine structure is not resolved in the ESR spectra. The fine-structure parameters are first found approximately from the magnetic-field positions of the ESR lines by using approximations to Eqs. (2) for the various magnetic-field directions in the crystals. The final values are obtained by varying each one

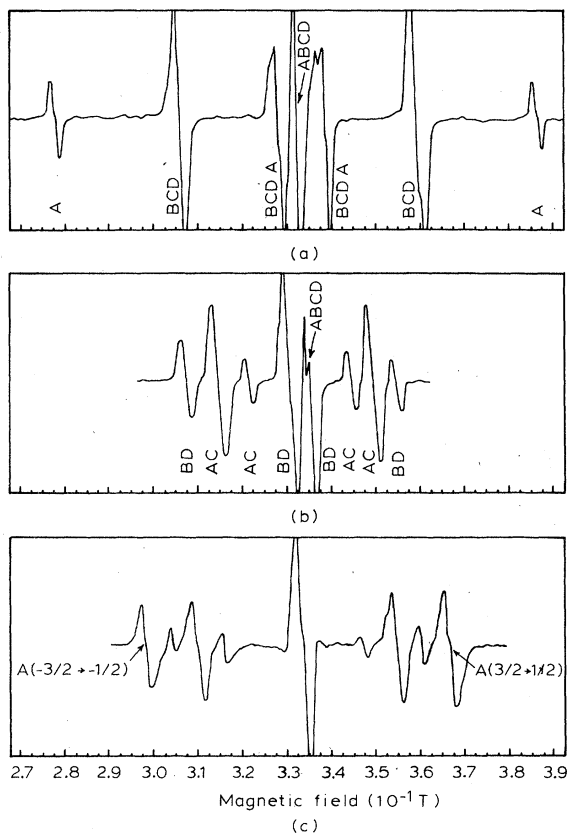


FIG. 1. ESR spectra of $^{57}\text{Fe}^{3+}$ in RbGa alum with H (a) along a $[111]$ axis, (b) on a $[1\bar{1}0]$ axis, and (c) near a cubic field axis in a (110) plane. A , B , C , and D refer to the four magnetic complexes in the unit cell.

separately in Eqs. (2), using a computer program until a best fit is obtained. The best-fit values for the two alums are listed in Table I.

B. ENDOR results

Locher and Geschwind² used the following terms in the spin Hamiltonian to describe the ENDOR

TABLE I. ESR and ENDOR spin-Hamiltonian parameters for $^{57}\text{Fe}^{3+}$ in $\text{RbAl}(\text{SO}_4)_2 \cdot 12\text{H}_2\text{O}$ and $\text{RbGa}(\text{SO}_4)_2 \cdot 12\text{H}_2\text{O}$ at 4.2 K.

Parameter	RbAl	RbGa	Error
g	2.003	2.003	± 0.001
a (10^{-4} cm^{-1})	133	133	± 4
D (10^{-4} cm^{-1})	- 31	- 84	± 2
F (10^{-4} cm^{-1})	4	4	± 2
A (10^{-4} cm^{-1})	- 10.77	- 10.76	± 0.01
B (10^{-4} cm^{-1})	- 10.74	- 10.74	± 0.01
U_{\parallel} (10^{-4} cm^{-1})	- 0.0070	0.0010	± 0.0003
U_{\perp} (10^{-4} cm^{-1})	- 0.0013	- 0.0016	± 0.0003
g_I (μ_N)	0.180	0.180	± 0.004
α (degrees)	9.5	9.5	± 0.5

hyperfine spectrum of $^{57}\text{Fe}^{3+}$ in MgO:

$$\mathcal{H}_N = \left\{ A - \frac{1}{5}U[3S(S+1) - 1] \right\} \vec{S} \cdot \vec{I} - g_I \mu_N \vec{H} \cdot \vec{I} + U(S_{\xi}^2 I_{\xi} + S_{\eta}^2 I_{\eta} + S_{\zeta}^2 I_{\zeta}). \quad (3)$$

The ξ , η , and ζ directions are along the cubic field axis of the MgO crystal. The last term in Eq. (3) must be rotated to the trigonal axes in the alums since the local symmetry is trigonal. Upon making Eq. (3) axially symmetric, the complete spin Hamiltonian is written in matrix form. In the procedure of fitting it to the ENDOR frequencies, equations correct to first order in perturbation theory are initially used to obtain approximate values of the hyperfine parameters. These values are then used as a starting point in the exact diagonalization of the matrix using an IMSL subroutine computer program.¹¹

ENDOR measurements on $^{57}\text{Fe}^{3+}$ in RbAl and RbGa alums were obtained with the magnetic field H parallel to a $[111]$ direction and near a cubic field axis. In these two directions small inaccuracies in orientation of the magnetic field are of least importance and the ENDOR lines have their strongest intensities. To obtain measurements near a cubic field axis the magnetic field was rotated by an angle of 9.5° from a $[100]$ direction in a (110) plane. This angle was determined from the ESR studies. ENDOR spectra were obtained along the two magnetic field directions for settings on the observed ESR lines for the four magnetic complexes. Some typical ENDOR spectra obtained for the case of RbGa alum are shown in Fig. 2. For H along a trigonal direction two sets of spectral lines, for complexes with $\theta = 0^\circ$ and 70.5° , were often observed. For H near a cubic field direction four sets of spectra due to the four inequivalent sites are observed. In some cases the spectral lines from different sites overlapped, and so their values could not be precisely determined. This introduced a systematic error in the measurement of these lines. For this reason, and also because of the low intensity of some lines, the accuracy of the ENDOR measurements was limited to 0.02 MHz. For H near a cubic field axis the $M_s = \pm \frac{5}{2}$ frequencies could be fitted most accurately to the spin Hamiltonian. This is because a misalignment of 1° in the direction of H produced a shift of 0.03 MHz for the $M_s = \pm \frac{3}{2}$ frequencies and much less for the $M_s = \pm \frac{5}{2}$ frequencies. All the ENDOR transitions observed from the four chromium magnetic complexes for a given magnetic field direction in the crystals were fitted to Eq. (3). The hyperfine-structure parameters obtained at best fit are listed in Table I. A graphical presentation of the fit for

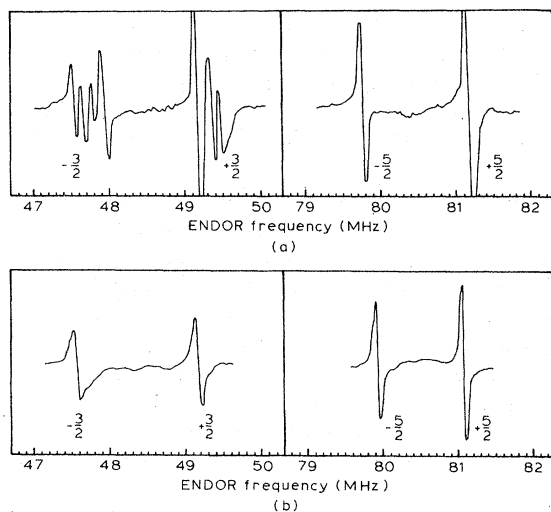


FIG. 2. ENDOR spectra of $^{57}\text{Fe}^{3+}$ in RbGa alum for (a) H near a cubic field axis and set on the $M_s = \frac{1}{2} \rightarrow -\frac{1}{2}$ ESR line, (b) H along a [111] direction and set on the $M_s = \frac{3}{2} \rightarrow \frac{1}{2}$ ESR line. The numbers $\frac{5}{2}, \frac{3}{2}$, etc., refer to the M_s values of the energy levels from where the transitions originate.

some typical frequencies measured in RbGa alum is given in Fig. 3.

III. DISCUSSION AND CONCLUSIONS

The fine-structure parameters obtained in this work are listed in Table II along with the results of Bleaney and Trenam.⁶ It is observed that the cubic field-splitting parameter a has nearly the same value in the alums, while the D parameter can vary greatly and be positive or negative. The Fe^{3+} D value is larger in RbGa than in RbAl alum. This was also found to be the case for the Cr^{3+} D value in the Rb alums.⁹ Hence the same situation exists even though the D values for Cr and Fe have opposite signs. It seems likely that this signifies that the trigonal crystal field at both the Fe^{3+} and Cr^{3+} sites is in extension in the Rb alums. It was found in the previous work⁹ that when a trigonal

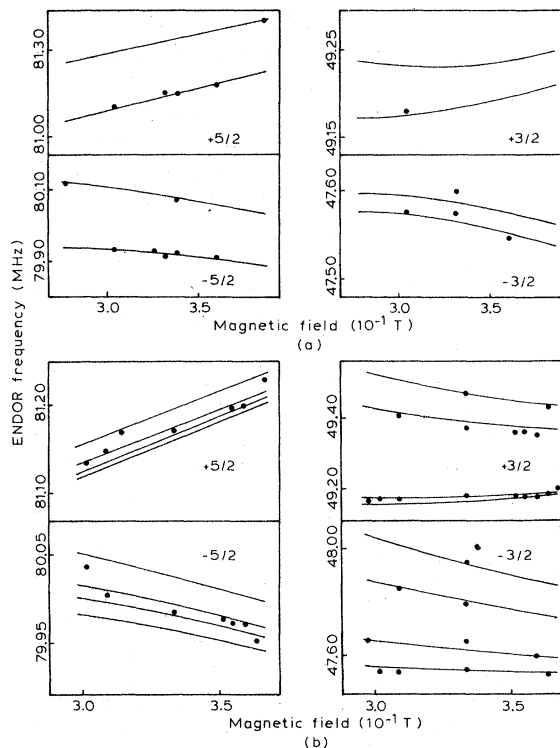


FIG. 3. Calculated (solid lines) and observed (solid points) ENDOR frequencies vs H obtained in RbGa alum for the magnetic field (a) along a [111] direction and (b) near a cubic field axis. The numbers $\frac{5}{2}, \frac{3}{2}$, etc., refer to the M_s values of the energy levels from where the transitions originate.

compression existed at a Cr^{3+} site, then the crystal isomorphs containing Ga possessed a smaller D value than those containing Al. This was found for Cr^{3+} in the Cs alums and the guanidium salts. As far as size considerations are concerned, Fe^{3+} and Cr^{3+} have nearly identical radii of $\sim 0.63 \text{ \AA}$, so the size effect will not complicate the comparisons.

Culvahouse and Olsen⁵ found a value of $|A| = (10.9 \pm 0.3) \times 10^{-4} \text{ cm}^{-1}$ for the hyperfine paramete-

TABLE II. Fine-structure parameters for Fe^{3+} in some alums. The number in parentheses is the error on the last digit.

Alum	Temperature (K)	a	Parameter (10^{-4} cm^{-1})		
			D	F	g
$\text{RbAl}(\text{SO}_4)_2 \cdot 12\text{H}_2\text{O}^a$	4.2	133(4)	- 31(2)	4(2)	2.003(1)
$\text{RbGa}(\text{SO}_4)_2 \cdot 12\text{H}_2\text{O}^a$	4.2	133(4)	- 84(2)	4(2)	2.003(1)
$\text{RbAl}(\text{SO}_4)_2 \cdot 12\text{H}_2\text{O}^b$	20	134(1)	- 31(1)	3(1)	2.003(1)
	90	134(2)	- 22(2)	3(2)	2.003(1)
$\text{KAl}(\text{SO}_4)_2 \cdot 12\text{H}_2\text{O}^b$	20	127(2)	115(1)	2(1)	2.003(1)
	90	127(2)	103(1)	2(2)	2.003(1)

^aThis work.

^bBleaney and Trenam, Ref. 6.

ter of $^{57}\text{Fe}^{3+}$ in double nitrate crystals using ordinary ESR. This is one of the few hydrated crystals in which resolution of the $^{57}\text{Fe}^{3+}$ hyperfine lines was reported. The values measured in the present work using ENDOR fall within the value found for the double nitrate, but the accuracy is improved by two significant figures. The values for A and B are nearly the same in the Rb alums, and any anisotropy in these parameters is minimal. Hence the small trigonal distortion existing in the Rb alums has little effect on the contribution of the $\vec{I} \cdot \vec{S}$ term in the spin Hamiltonian. Locher and Geschwind² found an isotropic value of $A = -10.059 \times 10^{-4} \text{ cm}^{-1}$ in MgO. As expected, this value is smaller than the ones found in the hydrated crystals because of the increased covalent bonding existing for the O^{2-} coordination in MgO.

The U_{\perp} parameter has nearly the same value in both the RbAl and RbGa alums but U_{\parallel} differs greatly. Hence the contribution of the S^2I term along a trigonal direction is affected by the trigonal distortion. In MgO it was found² that $U_{\parallel} = U_{\perp} = -0.0019 \times 10^{-4} \text{ cm}^{-1}$, and this is essentially identical to the value of U_{\perp} found in the present work. The nuclear g factor was found to be $g_I = 0.180\mu_N$ for the Rb alums, which is the same

as that found in MgO, but less accuracy is obtained in the present case due to broadened ENDOR lines in the hydrated environment. Accuracy is also lost in the alums because of overlapping of ENDOR lines from the four inequivalent sites.

It is useful to perform ENDOR measurements on the $^{57}\text{Fe}^{3+}$ ion in other crystals whether hydrated or not, and with large or small trigonal splittings, in order to classify their spin-Hamiltonian parameters. Such a classification would allow a better understanding of the physical behavior of the materials. Nicholson and Burns¹² attempted to classify some Fe^{3+} -doped crystals on the basis of the D value measured by ESR and the quadrupole coupling parameter measured using the Mössbauer technique. The results were only partially successful because the signs of the parameters were not known in many cases.

ACKNOWLEDGMENT

The authors would like to thank the National Research Council of Canada, Ottawa, Canada, for financial assistance during the course of this work.

¹A. Danilov and A. Manoogian, *Phys. Rev. B* **6**, 4097 (1972).

²P. R. Locher and S. Geschwind, *Phys. Rev.* **139**, 991 (1965).

³R. Calvo, M. C. G. Passeggi, and R. A. Isaacson, *Phys. Lett. A* **31**, 407 (1970).

⁴W. Rhein, *Z. Naturforsch. A* **27**, 741 (1972).

⁵J. W. Culvahouse and L. C. Olsen, *J. Chem. Phys.* **43**, 1145 (1965).

⁶B. Bleaney and R. S. Trenam, *Proc. R. Soc. Lond.*

A **223**, 1 (1954).

⁷S. Geschwind, *Phys. Rev. Lett.* **3**, 207 (1959).

⁸H. Watanabe, *Prog. Theor. Phys.* **18**, 405 (1957).

⁹A. Manoogian and A. Leclerc, *J. Chem. Phys.* **63**, 4450 (1975).

¹⁰S. Geschwind, *Phys. Rev.* **121**, 363 (1961).

¹¹*The IMSL Library* (International Mathematical Statistical Libraries Inc., Houston, 1975), Vol. 1.

¹²W. J. Nicholson and G. Burns, *Phys. Rev.* **129**, 2490 (1963).